Journal of Engineering and Technology for Industrial Applications

ISSN ONLINE: 2447-0228

ITEGAM-JETIA

Manaus, v.12 n.57, p. 416-427. January/February, 2026.

DOI: https://doi.org/10.5935/jetia. v12i57.3028

RESEARCH ARTICLE OPEN ACCESS

EXPERIMENTAL INVESTIGATION ON MICROSTRUCTURE AND MECHANICAL PROPERTIES OF SINTERED 316 STAINLESS STEEL SPECIMEN FOR BIO IMPLANTS

Imthiyas A*[1], Bubesh Kumar D[2], Sangeetha Krishnamoorthi S[3], Vasanth kumar J[4] and Dhanush kumar[5]

[1, 2, 3, 4, 5]Department of Mechanical Engineering, Aarupadai Veedu Institute of Technology, Vinayaka Mission's Research Foundation (DU), Tamil Nadu, India.

[1]https://orcid.org/0009-0002-1516-9426, [2]https://orcid.org/0000-0002-4308-2793, [3]https://orcid.org/0000-0003-1427-8743
[4]https://orcid.org/0009-0007-8563-6516, [5]https://orcid.org/0009-0004-8929-3379

Email: * imthiyas@avit.ac.in

ARTICLE INFO

Article History
Received: November 30, 2025
Revised: December 10, 2025
Accepted: January 1, 2026
Published: January 31, 2026

Keywords:
SS 316,
Plasma sintering,
Mechanical properties,
Biomedical,
Composites.

ABSTRACT

This project focuses on the experimental investigation of microstructural and mechanical behavior of sintered stainless steel 316 (SS316) under various processing and compositional conditions. SS316 metal powder with 99% purity and a particle size range of 30–45 microns were utilized in both advanced and conventional sintering techniques. The first phase involved Spark Plasma Sintering (SPS) at 950°C, with a pressure of 40 MPa and a dwell time of 10 minutes, producing dense and compact specimens. In the second phase, the metal powder was sintered using a conventional furnace after cold pressing at 10 kg/cm². Corrosion testing was conducted for 7 days in distilled water, seawater, and sodium hydroxide solutions to study degradation behavior. In the third phase, SS316 powder was reinforced with ceramic and non-metallic additives such as alumina, zirconia, hydroxyapatite, and silicon in different weight ratios (25–30%), followed by sintering in a muffle furnace at 900°C. This research aims to compare the microstructure, corrosion resistance, and mechanical performance of pure and reinforced SS316 under different sintering environments, offering insights into material selection for biomedical, structural, and corrosion resistant applications.

I. INTRODUCTION

Stainless Steel 316 (SS316) is a widely used austenitic stainless steel known for its excellent corrosion resistance, mechanical strength, and biocompatibility. It is extensively applied in marine environments, medical implants, and industrial processing due to its high chromium, nickel, and molybdenum content. In powder metallurgy, sintering of metal powders enables the fabrication of complex shapes and tailored microstructures with reduced waste and energy consumption [1] [2]. Biomedical implants and medical devices have become essential components of modern health care, offering significant improvements in comfort, mobility and overall life expectancy. As medical needs continue to expand, there is a growing demand for materials that can perform safely and reliably inside the human body. The creation of such materials requires careful control over physical, chemical and mechanical characteristics, since each implant must operate under complex biological conditions [3] [4]. Advances in material science directly influence the progress of implant manufacturing, leading to the design of components that are stronger, more compatible with human tissue and capable of long-term performance. The search for improved biomaterials therefore remains a central focus in current research, particularly in the development of metals and composites that combine mechanical strength with biological acceptance [5] [6]. Spark Plasma Sintering (SPS) provides significant processing advantages such as rapid heating and sintering, high densification within a short time, and minimal grain growth, making it highly suitable for fabricating advanced metallic materials [7] [8].

SS316 is an ideal candidate for such processing due to its excellent corrosion resistance, high strength, good ductility, and inherent biocompatibility, which make it suitable for structural and biomedical applications [9] [10]. Furthermore, the incorporation of ceramic and silicon-based reinforcements enhances the performance of SS316 by improving surface hardness, increasing wear resistance, and introducing beneficial bioactivity, particularly when hydroxyapatite is used as a reinforcing phase. These combined advantages make SPS-processed and reinforced SS316 a promising material system for high-performance engineering and biomedical applications [11] [12] [13]. Powder metallurgy is a manufacturing route in which metallic powders are compacted and subsequently consolidated through controlled heating to form dense, functional components. During the sintering stage, atoms migrate across particle boundaries, promoting strong interparticle bonding, reducing voids, and improving overall mechanical integrity [14]. Owing to its capability to achieve intricate geometries and customized material characteristics, this approach has become an essential method for producing high-performance parts across various engineering sectors [15].

SS316 is valued for its excellent durability, corrosion tolerance and compatibility with biological environments. Its alloying elements, namely chromium, nickel and molybdenum, provide strong resistance to localized corrosion, particularly pitting and crevice attack in chloride rich conditions such as seawater. These characteristics make SS316 a preferred material for demanding structural and biomedical applications [16] [17]. SS316 finds widespread use in marine, chemical and biomedical environments due to its reliable performance in corrosive conditions. The material can be effectively consolidated through powder metallurgy routes, and it responds well to the addition of reinforcing phases, making it a versatile option for developing advanced composite structures [18] [19].

Spark Plasma Sintering is an advanced consolidation method in which a pulsed direct current is applied together with external pressure to compact powders quickly and efficiently. The process is known for achieving very high density within a short duration, supported by extremely fast heating rates, lower required sintering temperatures and minimal grain coarsening. These features make SPS an effective technique for producing refined and high-performance materials [20].

Previous investigations show that the use of Spark Plasma Sintering can lead to stainless steel components with finer microstructural features and enhanced mechanical properties when compared to materials produced through conventional sintering routes. This improvement is attributed to the rapid and controlled consolidation conditions provided by the SPS process [8]. Conventional sintering is carried out by heating pressed metal powders in a furnace for a prolonged duration so that atomic diffusion can occur and the particles can join together. This approach often results in enlarged grains and may not always achieve full densification, particularly when very fine powders are used. In the case of SS316, reported processing temperatures typically fall between 900°C and 1200°C, and the resulting microstructure as well as the final properties are strongly influenced by both the selected temperature and the time for which the material is held at that temperature [2]. Microstructural features in sintered materials can be examined using Scanning Electron Microscopy, which offers detailed surface imaging at very high resolution. When combined with Energy Dispersive X Ray Spectroscopy, this technique also allows the identification of the elements present in different regions of the sample.

Together, these analytical tools make it possible to observe phases, detect pores and study the distribution of constituent elements, providing valuable insight into the quality of sintering and the uniformity of composite materials [21]. Sintered SS316 exhibits mechanical characteristics such as hardness, strength and ductility, all of which depend on factors like residual porosity, grain refinement and the conditions used during consolidation. Its resistance to corrosion in chloride rich and alkaline media is one of its major advantages, although material degradation can still occur when localized attack begins or when the protective surface film loses stability. These behaviors are important for evaluating the performance of SS316 in demanding service environments [22]. Improvements in consolidation conditions along with the addition of suitable reinforcing phases can lead to noticeable gains in the mechanical and corrosion related performance of the material [23]. The addition of ceramic phases to stainless steel, including materials such as alumina, zirconia and hydroxyapatite, is known to enhance properties like hardness, resistance to wear and stability at elevated temperatures. Hydroxyapatite also provides bioactive characteristics, which makes it attractive for medical related uses.

Reports in the literature indicate that incorporating ceramic content in the range of twenty to thirty percent can improve overall performance while still retaining the corrosion resistant nature of the steel matrix [24]. Silicon can act as an additional reinforcing phase because it offers high hardness and effective heat conducting ability. Its inclusion in the metal matrix contributes to improved strength and supports better overall structural performance [25]. This study explores the sintering behavior and performance of SS316 using both advanced and conventional approaches. While traditional furnace sintering is cost-effective, SPS offers rapid densification and improved control over grain structure due to its high heating rate and applied pressure. Additionally, combining SS316 with ceramic materials such as alumina, zirconia, hydroxyapatite, and silicon may enhance its hardness, corrosion resistance, and applicability in biomedical and high-temperature environments [26]. The outcomes of this work have relevance across several industrial sectors. In the biomedical field, SS316 composites reinforced with hydroxyapatite offer potential for bone implant and orthopaedic applications due to their biocompatibility and enhanced performance.

In marine environments, the excellent corrosion resistance of SS316 makes it suitable for underwater and offshore components. Aerospace and defense applications can benefit from high-strength, wear-resistant sintered composites that contribute to lightweight structural designs. Within the energy and nuclear sectors, SS316 is already widely deployed for reactor components, and improved composite versions can further enhance resistance to stress, wear, and corrosion under demanding service conditions.

The primary objective of this study is to fabricate SS316 sintered pellets using both SPS and conventional sintering techniques and to investigate how variations in particle size and sintering parameters influence the resulting density, microstructure, and mechanical properties of SS316. The work further aims to analyze the effects of ceramic and silicon-based reinforcements on the characteristics of the sintered composites. Additionally, corrosion behaviour is evaluated by subjecting the sintered SS316 specimens to different environments, including water, seawater, and NaOH. Comprehensive microstructural characterization is carried out using Scanning Electron Microscopy (SEM) coupled with Energy Dispersive X-ray Spectroscopy (EDX), and the hardness of both pure and reinforced SS316 samples is assessed to understand their performance enhancement.

II. MATERIALS AND METHODS

The primary raw material used in this work was SS 316 powder, selected for its corrosion resistance and suitability for consolidation through powder metallurgy routes. Table 1 shows the powder specifications used in the research work. The metal powder served as the main matrix for all specimens. To prepare composite variants, several reinforcing substances were incorporated. Alumina was employed for its high hardness and chemical stability. Zirconia was selected due to its toughness and compatibility with the steel matrix. Hydroxyapatite, which contains calcium and phosphate groups, was included to introduce bioactive characteristics that are valuable for biomedical applications. Silicon powder was added as an additional strengthening phase because of its hardness and ability to assist in heat transfer during processing. Ethanol was used during the mixing stage to assist in uniform blending of the powders and to act as a temporary binder. All powders were stored in sealed containers prior to use to prevent moisture absorption and contamination.

Table 1: Powder specifications.

Property	**Value**
Purity	99%
Particle size	30-45 microns
Gross weight	270 grams
Net weight	250 grams
Density	8.0 g/cm^3
Melting point	1400-1450°C

Source: Authors (2026).

The preparation of the sintered samples followed a systematic sequence beginning with the weighing of the required quantities of SS 316 powder and the selected reinforcement materials. Table 2 represents the parameters used in the SPS study. Each powder mixture was prepared according to the intended composition, ensuring that the chosen percentages of alumina, zirconia, hydroxyapatite and silicon were accurately maintained. Ethanol was added in small amounts to aid in achieving a uniform distribution of the reinforcing particles throughout the steel matrix.

Table 2: SPS parameters used in this study.

.**Parameters**		**Value**
Sintering temperature		950°C
Applied pressure		40 MPa
Heating rate		100°C/min
Holding time		10 min

Source: Authors (2026).

The powders were blended using a ball mill operated at controlled speed to prevent excessive heat generation or unwanted structural changes in the powder particles. The fig. 1 shows the powders used in this study. The milling process continued until a visually homogeneous mixture was obtained. The blended powders were then dried at moderate temperature to remove traces of ethanol before compaction.

(a) (b) (c)

Figure 1: (a) Stainless steel 316, (b) Al_2O_3 ZrO_2 $Ca_{10}(PO_4)_6(OH)_2$, and (c) Silicon.
Source: Authors (2026).

For pellet formation, the dried powder mixtures were placed into a steel die and compacted using a hydraulic press. A constant load was applied to produce green pellets with adequate strength for handling. These compacted samples were then subjected to thermal consolidation. A portion of the specimens was processed using SPS, where current assisted heating and pressure were applied simultaneously [26]. Another portion was consolidated by the traditional furnace sintering route, where pellets were placed in a controlled atmosphere furnace and heated at the target temperature for the selected holding time. After cooling, the samples were removed, labelled and stored for testing. Figure 2 shows the flowchart of the research work.

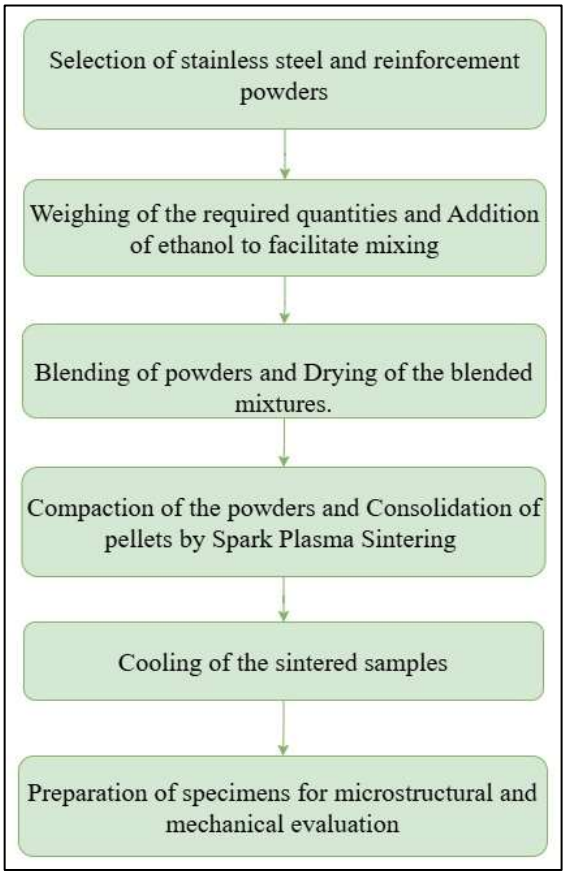

Figure 2: Flowchart of the work.
Source: Authors (2026).

A Spark Plasma Sintering system manufactured by Fuji was employed for the rapid consolidation of the prepared powders. This equipment is capable of reaching temperatures well above 1000°C and can apply pressures to 40 MPa [8]. Figure 3 represents the SPS image used for this study. The system allows the simultaneous application of electrical current and mechanical load, enabling fast heating and effective densification of the compacted samples.

Figure 3: SPS Instrument.
Source: Authors (2026).

A muffle furnace was used for the conventional sintering route. Figure 4 (a), (b) represents the muffle furnace and manual pellet press used in this study. This furnace provided controlled and uniform heating for extended durations, allowing pellets to be consolidated through traditional thermal treatment. The heating chamber offered stable temperature distribution, which is essential for consistent microstructural development.

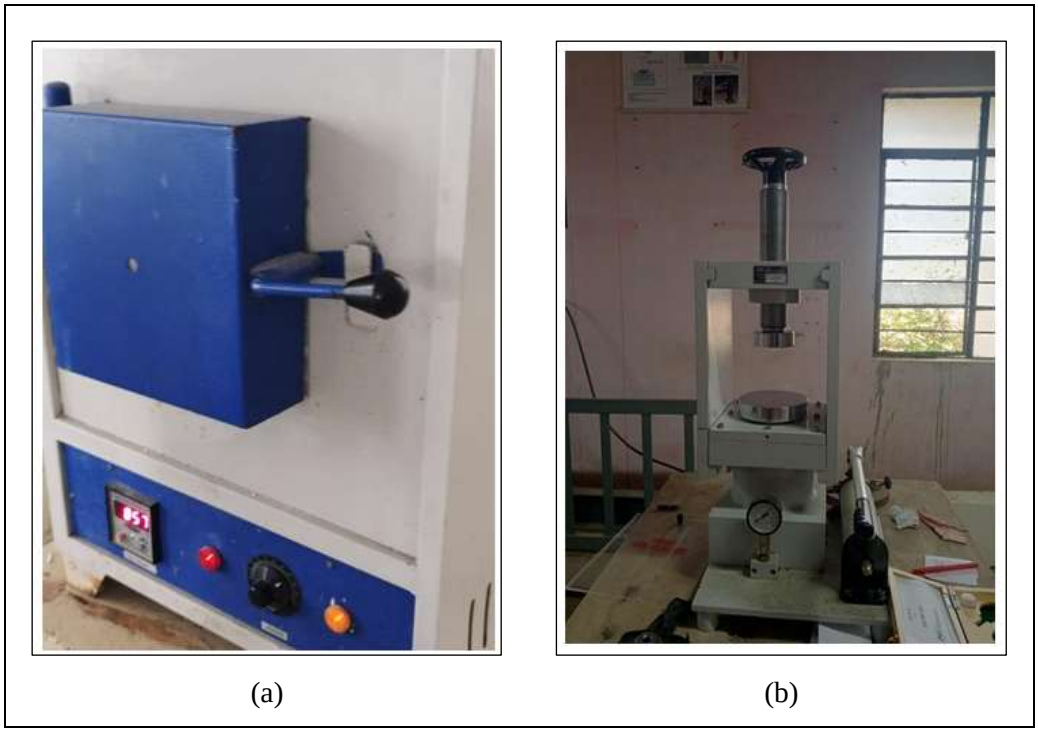

(a) (b)

Figure 4: (a) Muffle furnace and (b) Pallet press.
Source: Authors (2026).

The preparation of the pellet using SPS began with the measurement of 10g of SS 316 powder. The selected quantity was placed in a clean container and transferred into the die set that belongs to the Fuji Spark Plasma Sintering system. Figurer 5 shows the pellet made from the sintering. The sintering operation was carried out under controlled settings. These conditions were selected to promote rapid consolidation while preventing unnecessary grain growth. After the heating cycle, the pellet was allowed to cool inside the chamber. The final compact had a diameter of approximately 10 mm and a thickness of 4 mm. Once the pellet was released from the die, it was weighed, and any unutilized powder was collected for reuse.

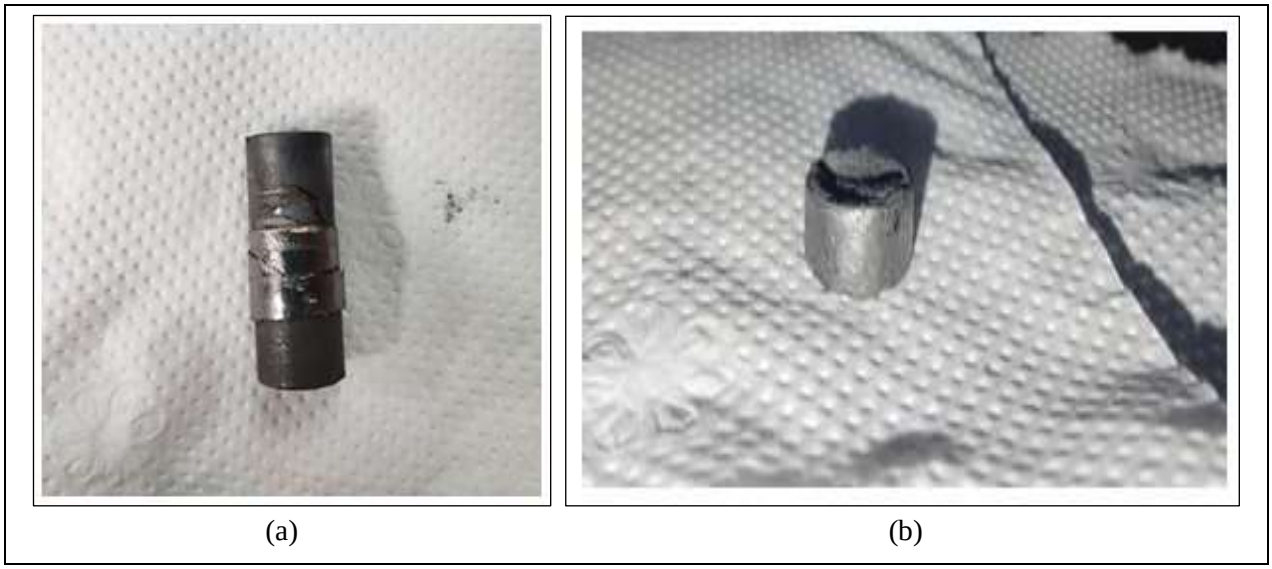

(a) (b)

Figure 5: (a) Pallet with die and (b) Pallet.
Source: Authors (2026).

The surface of the sintered pellet was prepared to make it suitable for microstructural evaluation. A series of abrasive papers was used in sequence beginning with grade 0/3, followed by 0/2, 0/1 and finally E 120. This progression helped in removing surface irregularities and oxidation products. After the sanding stage, the specimen was transferred to a double disc polishing unit. Alumina paste was applied to the rotating surface of the polishing machine, and the pellet was gently pressed against the disc until a smooth and reflective finish was obtained. The polished specimen was rinsed thoroughly with clean water to remove any remaining abrasive particles. The resulting surface exhibited a bright mirror like appearance, which ensured clear microscopic imaging. The polished pellet produced through SPS was forwarded for microstructural and elemental examination. The SEM was used to observe pore distribution, grain boundaries and the overall surface features of the material. The same instrument was equipped with an energy dispersive X ray unit which enabled the identification of the elements present in the examined regions. This allowed verification of the chemical uniformity of the SS 316 sample. A separate set of pellets was prepared using the traditional route.

One gram of SS powder was placed inside a steel die and compressed using a manually operated press. A load of 10 g/cm2 was applied for 30 seconds to form compact samples. Three pellets were produced in this manner. Each compact had an average thickness of 3 mm and a diameter of 10 mm. The green pellets were placed inside a muffle furnace and heated to 900°C for 10 minutes. Once the heating cycle was completed, the furnace was switched off and allowed to cool naturally for 12 hours. This slow cooling reduced thermal stress in the samples. Three individual pellets were immersed in different media to evaluate their corrosion behaviour. One beaker contained distilled water, the second contained seawater, and the third contained a mixture prepared by dissolving 1.3g of sodium hydroxide in 30 mm of water. The pellets remained in these media for 8 days. Their mass and visible surface condition were recorded before and after the exposure period. Three composite formulations were prepared shown in Table 3.

Table 3: Composite sample details.

Mixture No.	Sample composition	Time Held
Mixture 1	75% SS316 + 25%	60 seconds
Mixture 2	70% SS316 + 30%	120 seconds
Mixture 3	70% SS316 + 30%	120 seconds

Source: Authors (2026).

Ethanol was added during mixing to help distribute the additives uniformly. The powders were blended manually in a grinding bowl until a consistent mixture was obtained. The prepared mixtures were pressed into pellets using the manual press. A load of 15 kg/cm2 was maintained for each pellet. The holding time was 60 seconds for the mixtures with ceramic additives and 120 seconds for the mixture that contained silicon. This ensured adequate green strength for handling [27]. All composite pellets were heated in the muffle furnace at 900°C for 15 minutes. They were then allowed to cool slowly inside the furnace for 12 hours. This natural cooling prevented cracking and maintained structural stability [20]. After processing, all composite pellets were submitted for hardness measurement. The cold compaction of powder mixtures was carried out using a manually operated pallet press. This press generated the required load to form green pellets with sufficient strength for further processing. The die set used in the press ensured that all samples were produced with identical size and shape. Surface preparation of the sintered specimens was performed using a double disc polishing machine.

This device enabled the removal of surface irregularities and produced a smooth finish suitable for microstructural examination. A series of abrasive papers was used during this process, including grades ranging from coarse to fine such as 0/3, 0/2, 0/1 and E 120. Each grade allowed gradual refinement of the sample surface before final polishing. Microstructural analysis was carried out using a scanning electron microscope equipped with an energy dispersive X ray system. The microscope provided high resolution imaging to observe features such as grain structure, pore distribution and reinforcement dispersion. The attached energy dispersive system enabled elemental analysis of selected regions, helping to confirm the presence and distribution of ceramic and silicon-based phases in the composite samples. Mechanical characterization was performed using a hardness testing machine. This instrument applied a controlled load to the polished specimen surface and measured the resulting indentation, providing an indication of the resistance of the material to localized deformation. Hardness values were used to compare pure SS pellets with those containing reinforcing phases.

III. RESULTS AND DISCUSSION

The SS 316 powder that was processed through the SPS route produced a compact pellet with clear evidence of effective consolidation. The rapid heating combined with the applied pressure resulted in strong bonding among the particles, and the final compact retained its shape without visible cracks or structural distortion. The compact had a diameter of 10 mm and a thickness of 4 mm after sintering. The recorded mass of 2.532g after the heating cycle indicated that the loss of material during the process was very small. The sintering temperature was maintained at 950°C, with an applied pressure of 40 MPa and a holding duration of 10 minutes.
These measured values point to a high degree of densification. Fig 6 represents the SEM image of the samples. The consistency in dimensions before and after processing suggests that the applied pressure and controlled temperature cycle enabled the SS 316 particles to rearrange and bond efficiently. The absence of significant mass reduction further confirms that the consolidation took place without major oxidation, evaporation or powder ejection.

Such results illustrate the capability of the SPS method to produce dense metallic pellets in a relatively short processing time when compared with conventional thermal treatments [28]. The overall outcome demonstrates that the selected sintering conditions were suitable for stainless steel grade, producing a compact with adequate density and structural stability. This provides the basis for further characterization such as microstructural analysis and hardness evaluation. The surface of the Spark Plasma Sintered SS 316 pellet was examined using SEM. The micrograph displayed a compact structure in which the particles had fused effectively, resulting in a surface with very little visible porosity. The arrangement of grains appeared consistent across the observed area, and the boundaries between adjacent grains were clearly identifiable [29]. The limited enlargement of these grains is expected, as the SPS technique employs rapid heating and a short exposure time at the peak temperature. This prevents excessive diffusion and restricts the growth of the individual grains. The surface did not show noticeable cracks, voids or defects, indicating that the consolidation process produced a stable and well bonded structure [30].

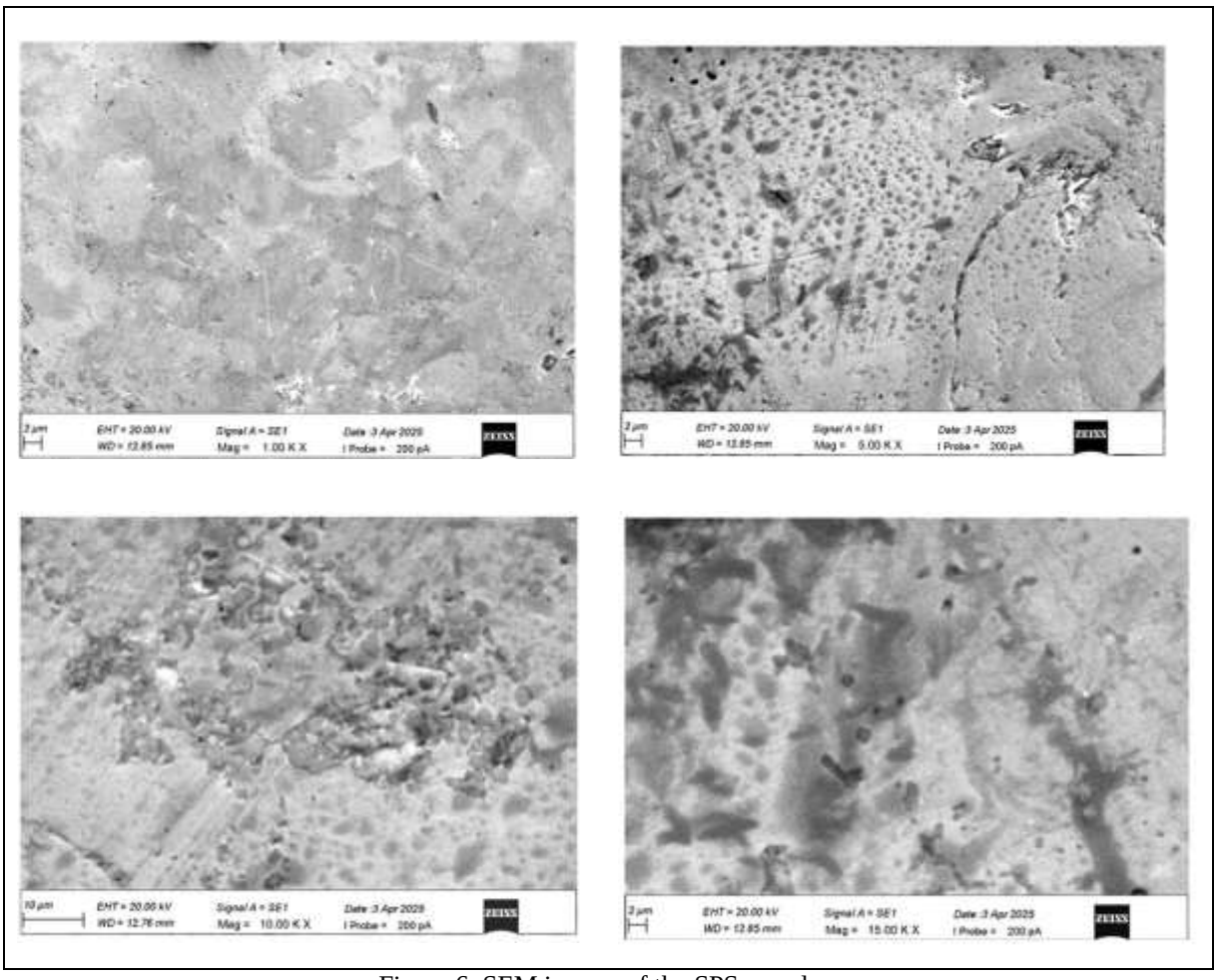

Figure 6: SEM images of the SPS samples.
Source: Authors (2026).

The microstructural features revealed through the microscopy confirm the advantages often associated with the SPS process. The presence of fine grains and the absence of large pores suggest that the material experienced efficient densification while avoiding the high degree of diffusion that typically occurs during long furnace treatments. The controlled grain size and dense structure are expected to have a positive influence on the mechanical performance of the pellet, particularly its hardness and resistance to surface deformation. Furthermore, the refined surface features and minimal oxidation indicate that the material will likely maintain favourable corrosion behaviour when exposed to aggressive environments [31]. Overall, the observed microstructure supports the conclusion that the chosen processing conditions were effective for producing a well consolidated SS sample.

Energy dispersive X ray examination was carried out at two selected regions of the Spark Plasma Sintered pellet. Figure 7 and 8 represents the EDX area 1 and 2 with the elemental mapping. The spectra from both regions presented clear and well resolved peaks corresponding to the elements that are normally present in stainless steel grade three hundred and sixteen. In the first region, elements such as carbon, oxygen, aluminium, silicon and titanium were detected in addition to the major constituents chromium, manganese, iron and nickel [1]. The presence of oxygen is attributed to slight surface oxidation during polishing, which is commonly observed in stainless steels when exposed to air. The second region displayed a composition dominated by chromium and iron, with smaller contributions from carbon and manganese.

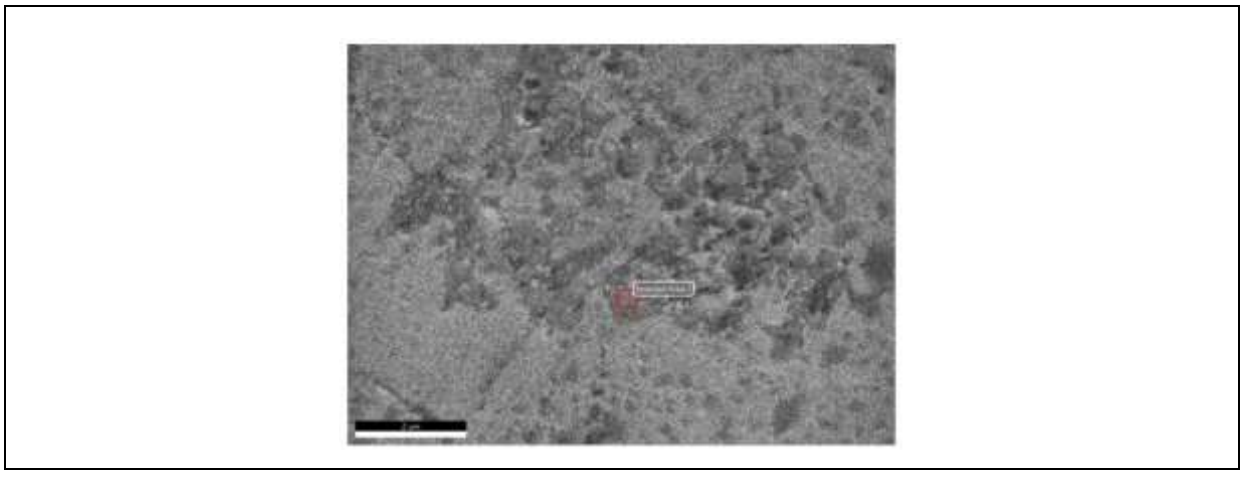

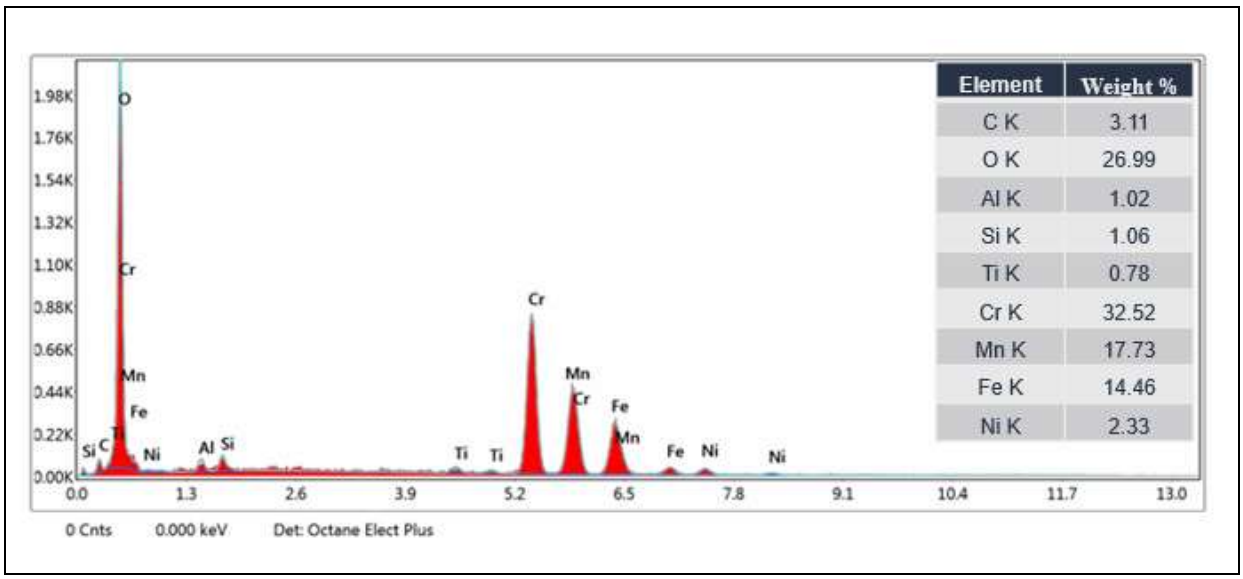

Figure 7: EDX area 1.
Source: Authors (2026).

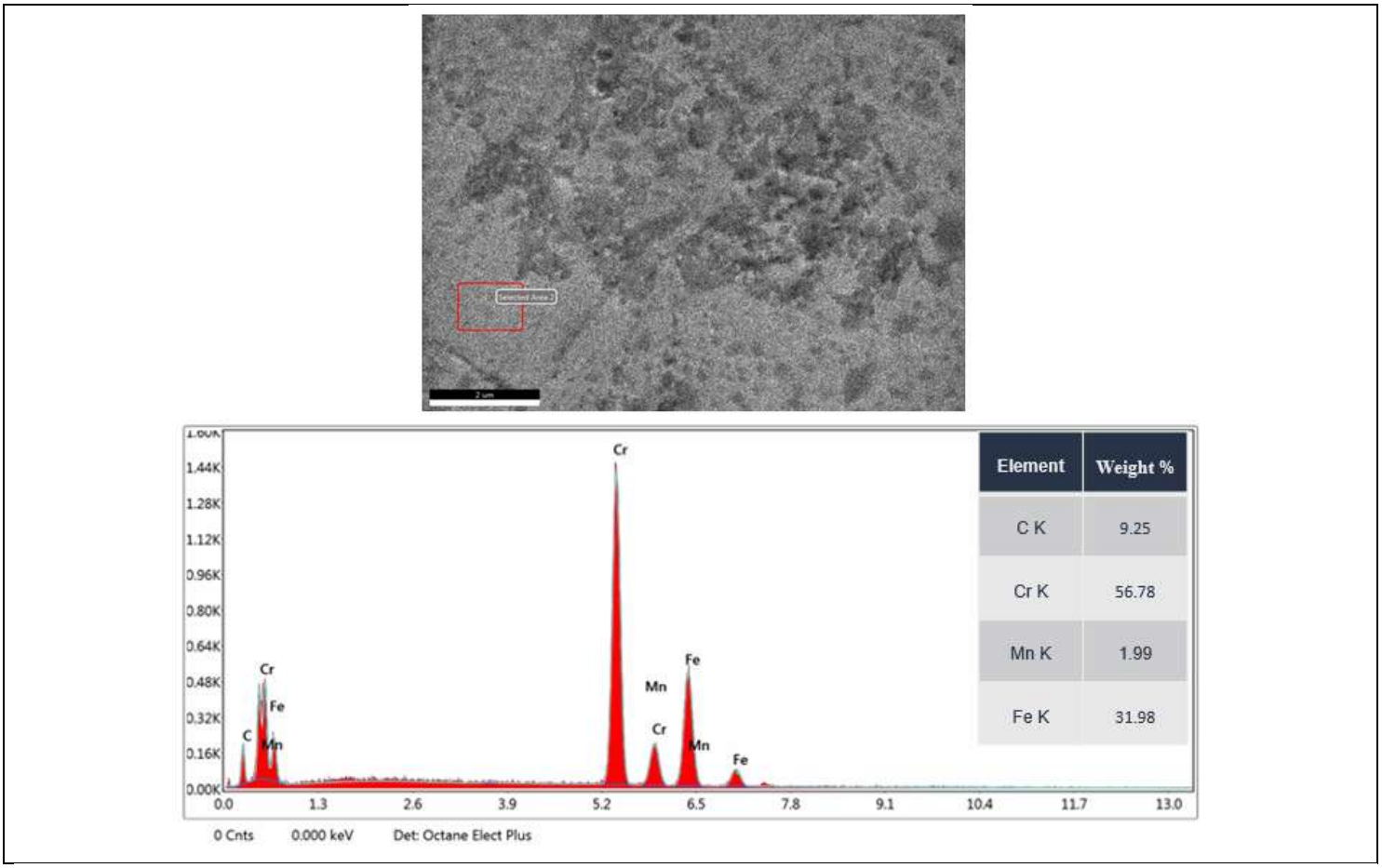

Figure 8: EDX area 2.
Source: Authors (2026).

The elemental concentrations observed in both regions fall within the expected range for stainless steel grade three hundred and sixteen. The detection of chromium, manganese, iron and nickel in appropriate proportions confirms that the alloy composition remained stable throughout the sintering process. The occasional presence of aluminum, silicon and titanium in the first region is attributed to minor traces left during surface preparation and does not indicate contamination of the bulk material [2]. The consistency in the distribution of the primary alloying elements across the examined regions demonstrates that the SPS method facilitated proper mixing and retention of the chemical composition. The process conditions prevented oxidation of the internal structure and avoided any loss of metallic constituents. The uniform chemical profile also supports the microstructural observations, showing that the rapid heating and controlled atmosphere of the sintering technique help maintain the integrity of the stainless steel powder during consolidation [7]. The combined results from both microstructural and elemental evaluation confirm that the sintered pellet preserved its intended composition.

No foreign substances or undesirable phases were detected, showing that the preparation and processing steps were performed without introducing impurities. The even distribution of chromium and iron, in particular, indicates that the corrosion resistant nature of the alloy is expected to be maintained in the final compact. These findings reinforce the reliability of the SPS route for producing dense SS 316 samples with stable chemical characteristics. Three pellets were produced through cold pressing followed by furnace sintering. All samples had a diameter of 10 mm and a thickness of 3 mm after compaction. Their appearance after the thermal cycle revealed slight variations that reflect the influence of traditional sintering conditions [23]. The first pellet maintained a stable shape and displayed a faint brown surface tint. This colour change is commonly associated with mild surface oxidation that forms during heating in a muffle furnace. The second pellet showed a very small reduction in size, suggesting a moderate level of shrinkage due to particle rearrangement and bonding during the heating stage. The third pellet exhibited a slightly uneven surface, indicating that the particle fusion was not completely uniform. Such surface roughness is typical when fine SS 316 powders are sintered without applied pressure [32].

The long cooling period of nearly 12 hours inside the furnace allowed the samples to return to room temperature gradually. This slow cooling helped reduce thermal stresses and promoted steady phase development within the material. It also prevented cracking, which is sometimes observed when metallic pellets are cooled abruptly. The visual and dimensional characteristics of the pellets confirm the expected behaviour of SS 316 during conventional furnace sintering. Compared with the Spark Plasma Sintered pellet, these samples show evidence of lower densification, as indicated by minor shrinkage and surface irregularities [33]. The appearance of oxidation on the surface also aligns with the furnace atmosphere, which does not offer the same level of control as vacuum based sintering processes. Overall, the results demonstrate that while conventional sintering can produce reasonably compact pellets, the degree of densification and surface quality is influenced strongly by furnace atmosphere, heating duration and absence of external pressure. These observations highlight the contrast between rapid current assisted consolidation and traditional thermal processing.

III.1 CORROSION BEHAVIOUR

The pellets produced through the conventional sintering route were immersed in three different media to examine their corrosion behaviour. The weights recorded before and after the 8-day exposure period is listed in Table 4. All samples showed a measurable reduction in mass, although the extent of loss differed depending on the environment.

Table 4: variation of weights.

Environment	Initial weight (g)	Final weight (g)	Change (g)	Remarks
Distilled Water	58.598	52.246	6.352	Minor expected
Sea Water	62.278	56.455	5.823	Possible pitting
NaOH Solution	65.911	61.181	4.73	Alkaline corrosion

Source: Authors (2026).

The pellet placed in distilled water lost 6.352 grams during the test. Distilled water contains no dissolved salts or aggressive ions, so the weight loss is attributed mainly to mild surface reactions and the removal of loosely bonded oxides. The pellet exposed to seawater lost 5.823 grams. Although the total mass loss is slightly lower compared with distilled water, the surface of this pellet is expected to show signs of localized attack caused by chloride ions. The sample immersed in the sodium hydroxide solution lost 4.73 grams. The alkaline nature of the medium often leads to the formation of surface films that can either protect or deteriorate depending on the material [34]. The reduction in mass in this case indicates that the film was unable to fully prevent the reaction between the pellet and the solution. The general trend observed in the weight measurements aligns with the expected behaviour of SS 316. The sample in distilled water experienced only mild degradation, confirming that SS 316 is largely stable in neutral environments. The seawater sample was subjected to chloride ions, which are known to disrupt the passive oxide layer that protects stainless steel.

This can lead to localized pits even if overall mass loss appears moderate [35]. The presence of such ions makes seawater a more aggressive medium despite the slightly lower numerical weight change [20] [36] . The specimen in the sodium hydroxide solution reacted with the alkaline medium. Although SS 316 shows some resistance in alkaline solutions, prolonged contact can still weaken the passive film and produce surface dullness or localized thinning. The mass loss recorded for this pellet indicates that the reaction rate was not negligible. These findings demonstrate that the corrosion resistance of the conventionally sintered pellets varies significantly with the nature of the environment. Neutral water causes minimal damage, seawater introduces the possibility of pitting through chloride action and the sodium hydroxide solution encourages surface layer disruption. The results also highlight the influence of sintering method on corrosion performance, since pellets produced without external pressure and rapid heating tend to contain surface irregularities that can further accelerate attack.

III.2 COMPOSITE SAMPLES OF REINFORCED STAINLESS STEEL

Three composite pellets were produced by introducing different reinforcing phases into stainless steel. The first composite, labelled C1, contained 75 % SS and 25 % of a combined mixture of alumina, zirconia and hydroxyapatite. This sample developed a uniform surface after sintering and showed no visible cracking. The second composite, labelled C2, contained 70 % SS and 30 % SS of the same ceramic mixture. This pellet also displayed a smooth surface but showed signs of increased rigidity due to the higher ceramic content. The third composite, labelled C3, was prepared with 70 % SS and 30 % silicon powder as shown in Table 5. This sample appeared dense but revealed a slightly brittle character after sintering, which is consistent with the presence of silicon rich phases that tend to limit ductility [27] [37] [38].

Table 5: Composite weight percentage with sintered temperature.

Sample ID	Composition	Sintered Temp	Time	Pressure	Remarks
C1	SS316 (75%) + Al_2O_3, ZrO_2, HA (25%)	900°C	15 min	15 kg/cm²	Clean surface
C2	SS316 (70%) + Al_2O_3, ZrO_2, HA (30%)	900°C	15 min	15 kg/cm²	Slightly brittle
C3	SS316 (70%) + Silicon (30%)	900°C	15 min	15 kg/cm²	Dense and hard sample

Source: Authors (2026).

The applied load for all compactions was fifteen kilogram per square centimeter, ensuring that the green pellets had enough strength to withstand handling and the subsequent thermal treatment. Hardness values were obtained for each of the composite pellets to evaluate the effect of reinforcement on mechanical strength. The data are summarized in Table 6.

Table 6: Hardness results.

Sample ID	Composition	Hardness (HV)	Remarks
C1	SS316 (75%) + Al_2O_3, ZrO_2, HA (25%)	539.3	Moderate hardness
C2	SS316 (70%) + Al_2O_3, ZrO_2, HA (30%)	380.3	Higher ceramic effect
C3	SS316 (70%) + Silicon (30%)	281.5	Possibly highest

Source: Authors (2026).

The pellet with 25% ceramic reinforcement, C1, recorded a hardness of 539.3 HV. This value indicates that the addition of the ceramic blend contributed significantly to resistance against localized deformation. The second pellet, C2, which contained a higher proportion of ceramic reinforcement, showed a hardness of 380.3 HV. Although still higher than unreinforced stainless steel, the reduction compared with C1 suggests that an excessive number of ceramic particles may have influenced the bonding between the steel matrix and the reinforcement, leading to reduced compactness [36] [39]. The third sample, C3, which contained silicon as the reinforcing phase, recorded a hardness of 281.5 HV. This lower value reflects the influence of silicon, which, although beneficial for strength improvements in some alloys, can form brittle phases during sintering that do not contribute positively to indentation resistance. The slightly brittle nature observed in C3 further supports this behaviour.

The comparison of the hardness values shows that the ceramic mixture of alumina, zirconia and hydroxyapatite was more effective in improving the mechanical resistance of the SS matrix compared with silicon. The moderate hardness obtained for C1 suggests an optimal balance between ceramic content and matrix consolidation, whereas the decreased hardness in C2 indicates that increasing ceramic content beyond a certain level may introduce porosity or reduce the bonding efficiency [40]. The silicon reinforced pellet exhibited the lowest hardness among the composites, implying that the structure formed during sintering may not support strong load transfer between the matrix and the reinforcing particles [41]. These results emphasize the importance of reinforcement type and composition in determining the final mechanical properties of powder consolidated materials [34].

IV. DISCUSSION

The results obtained from the Spark Plasma Sintered sample demonstrate the effectiveness of this consolidation technique in producing dense metallic pellets with refined microstructural features. The compact exhibited a smooth surface, limited porosity and clearly defined grain boundaries. Such features indicate efficient bonding between the SS 316 particles and suggest that the material would display strong mechanical behaviour, particularly in hardness and resistance to surface deformation [28]. The controlled thermal cycle of the SPS process appears to have played a major role in achieving these favourable characteristics. In contrast, the pellets prepared through the conventional furnace route displayed small variations in appearance and surface quality. Slight shrinkage, mild oxidation and uneven surface regions were observed.These outcomes are consistent with the nature of furnace sintering, where slower heating rates and the absence of applied pressure limit the extent of densification.

Even so, the pellets retained sufficient structural integrity to proceed with corrosion and mechanical evaluation. Their behaviour under different chemical environments provides valuable insight into the performance of SS 316 when processed using a more traditional approach. The composite samples developed with ceramic and silicon reinforcements displayed noticeably different hardness values, confirming that the type and amount of the reinforcing phase strongly influence the final mechanical response. The combination of alumina, zirconia and hydroxyapatite contributed to higher hardness compared with the silicon-based composite, demonstrating the effectiveness of ceramic additions in improving load bearing capability. The slight brittleness observed in the silicon reinforced material suggests that the formed structure may not support strong stress transfer within the matrix.

The corrosion test results further highlight the importance of processing technique and reinforcement content in determining the chemical stability of the pellets. Differences in mass loss among the samples immersed in distilled water, seawater and sodium hydroxide solutions show that the method of sintering influences surface quality and passive layer formation. The interaction of reinforcement phases with aggressive media will also help identify which composite formulation offers the most favourable balance between mechanical strength and environmental resistance. Taken together, the findings show that SPS provides superior densification and microstructural refinement, ceramic reinforcements enhance hardness and environmental exposure reveals the durability of the produced materials. These observations create a clear connection between processing conditions, microstructure and final performance.

V. CONCLUSIONS

The investigation shows that stainless steel 316 processed through powder metallurgy responds strongly to the choice of sintering technique and reinforcement strategy.

The SPS route delivered the most favourable outcome, producing a compact with very high density, smooth surface finish and a fine microstructure with minimal porosity. Elemental analysis confirmed that the chemical composition remained stable, indicating that the rapid current assisted heating preserved alloy integrity. These results position the SPS method as the most effective route in this study. The furnace sintered samples displayed moderate bonding and predictable mass loss during corrosion testing. Among the exposure conditions, seawater produced the most pronounced degradation due to chloride activity, while distilled water showed minimal effect. The alkaline solution caused surface film changes but lower mass loss compared with the salt environment.

The reinforced composites demonstrated clear variations in hardness. The mixture containing twenty five percent ceramic reinforcement produced the highest hardness value, indicating improved resistance to deformation. The silicon-based composite displayed lower hardness and a slightly brittle character, showing that reinforcement type has a significant impact on mechanical response. Future work should extend the mechanical evaluation to tensile and compression behaviour, explore thermal and electrical properties and optimize sintering conditions for even greater densification. Additional characterization through X ray diffraction, transmission electron microscopy and biological testing for hydroxyapatite-based composites will help establish the full potential of these material systems.

VI. AUTHOR'S CONTRIBUTION

Conceptualization: Imthiyas A, Bubesh Kumar D and Sangeetha Krishnamoorthi S.
Methodology: Imthiyas A, Bubesh Kumar D.
Investigation: Imthiyas A, Bubesh Kumar D.
Discussion of results: Imthiyas A, Bubesh Kumar D .
Writing – Original Draft: Imthiyas A.
Writing – Review and Editing: Imthiyas A , Bubesh Kumar D , Sangeetha Krishnamoorthi S , Vasanth kumar J and Dhanush kumar.
Resources: Imthiyas A.
Supervision: Bubesh Kumar D and Sangeetha Krishnamoorthi S.
Approval of the final text: Imthiyas A, Bubesh Kumar D and Sangeetha Krishnamoorthi S, Vasanth kumar J and Dhanush kumar.

VII. REFERENCES'

[1]F. L. Serafini et al., "Materials Characterization Microstructure and mechanical behavior of 316L liquid phase sintered stainless steel with boron addition," Mater. Charact., vol. 152, no. October 2018, pp. 253–264, 2019, doi: 10.1016/j.matchar.2019.04.009.

[2]S. Nitriding et al., "Optimization of Sintering Parameters of 316L Stainless Steel for In-Situ Nitrogen Absorption and," pp. 1–20, 2020.

[3]S. Ali, A. Majdi, A. Rani, Z. Baig, S. W. Ahmed, and G. Hussain, "Biocompatibility and corrosion resistance of metallic biomaterials," vol. 38, no. 5, pp. 381–402, 2020.

[4]M. Kaur and K. Singh, "Review on titanium and titanium-based alloys as biomaterials for orthopaedic applications," Mater. Sci. Eng. C, vol. 102, no. February, pp. 844–862, 2019, doi: https://doi.org/10.1016/j.msec.2019.04.064.

[5]A. Moridi, "Biomedical Applications of Metal Additive Manufacturing: Current State-of-the-Art and Future Perspective," Am. J. Biomed. Sci. Res., vol. 7, no. 1, pp. 6–10, 2020, doi: 10.34297/ajbsr.2020.07.001103.

[6]J. Ni et al., "Three-dimensional printing of metals for biomedical applications," Mater. Today Bio, vol. 3, no. August, 2019, doi: 10.1016/j.mtbio.2019.100024.

[7]A. B. Kale, B. Kim, D. Kim, E. G. Castle, M. Reece, and S. Choi, "Materials Characterization An investigation of the corrosion behavior of 316L stainless steel fabricated by SLM and SPS techniques," Mater. Charact., vol. 163, no. February, p. 110204, 2020, doi: 10.1016/j.matchar.2020.110204.

[8]E. Hug, C. Folton, J. Papin, K. Tabalaiev, and G. Marnier, "Ultrafine Grain 316L Stainless Steel Manufactured by Ball Milling and Spark Plasma Sintering : Consequences on the," 2024.

[9]Z. Zhan and H. Li, "Machine learning based fatigue life prediction with effects of additive manufacturing process parameters for printed SS 316L," Int. J. Fatigue, vol. 142, no. July 2020, p. 105941, 2021, doi: 10.1016/j.ijfatigue.2020.105941.

[10]M. Al-Amin et al., "Analysis of hybrid HA/CNT suspended-EDM process and multiple-objectives optimization to improve machining responses of 316L steel," J. Mater. Res. Technol., vol. 15, pp. 2557–2574, 2021, doi: 10.1016/j.jmrt.2021.09.074.

[11]H. Tetsuka and S. R. Shin, "Materials and technical innovations in 3D printing in biomedical applications," J. Mater. Chem. B, vol. 8, no. 15, pp. 2930–2950, 2020, doi: 10.1039/d0tb00034e.

[12]L. F. Velásquez-García and Y. Kornbluth, "Biomedical Applications of Metal 3D Printing," Annu. Rev. Biomed. Eng., vol. 23, pp. 307–338, 2021, doi: 10.1146/annurev-bioeng-082020-032402.

[13]W. Wang et al., "3D printing of PLA/n-HA composite scaffolds with customized mechanical properties and biological functions for bone tissue engineering," Compos. Part B Eng., vol. 224, no. July, p. 109192, 2021, doi: 10.1016/j.compositesb.2021.109192.

[14]S. M. Yusuf and N. Gao, "Influence of energy density on metallurgy and properties in metal additive manufacturing," Mater. Sci. Technol. (United Kingdom), vol. 33, no. 11, pp. 1269–1289, 2017, doi: 10.1080/02670836.2017.1289444.

[15]G. Iacob, V. G. Ghica, M. Buzatu, T. Buzatu, and M. Ionut, "Composites : Part B Studies on wear rate and micro-hardness of the Al / Al 2 O 3 / Gr hybrid composites produced via powder metallurgy," vol. 69, pp. 603–611, 2015, doi: 10.1016/j.compositesb.2014.07.008.

[16]H. Li, M. Ramezani, M. Li, C. Ma, and J. Wang, "Tribological performance of selective laser melted 316L stainless steel," Tribol. Int., vol. 128, no. April, pp. 121–129, 2018, doi: 10.1016/j.triboint.2018.07.021.

[17]V. Vishnu, T. R. Prabhu, M. Imam, and K. P. Vineesh, “Experimental Investigation into the Dry Reciprocating Wear Behavior of Additively Manufactured Austenitic Stainless Steel (316L) Alloys,” Jom, vol. 76, no. 6, pp. 3081–3098, 2024, doi: 10.1007/s11837-024-06491-9.

[18]S. N. Alam and L. Kumar, “Mechanical properties of aluminium based metal matrix composites reinforced with graphite nanoplatelets,” Mater. Sci. Eng. A, vol. 667, pp. 16–32, 2016, doi: 10.1016/j.msea.2016.04.054.

[19]P. Samal, P. R. Vundavilli, A. Meher, and M. M. Mahapatra, “Recent progress in aluminum metal matrix composites: A review on processing, mechanical and wear properties,” J. Manuf. Process., vol. 59, no. September, pp. 131–152, 2020, doi: 10.1016/j.jmapro.2020.09.010.

[20]E. Hug and C. Keller, “Passivation properties of ultrafine grain 316L stainless steels manufactured by ball milling and spark plasma sintering,” Mater. Chem. Phys., vol. 309, no. August, p. 128398, 2023, doi: 10.1016/j.matchemphys.2023.128398.

[21]K. Ravi Kumar, T. Pridhar, and V. S. Sree Balaji, “Mechanical properties and characterization of zirconium oxide (ZrO2) and coconut shell ash(CSA) reinforced aluminium (Al 6082) matrix hybrid composite,” J. Alloys Compd., vol. 765, pp. 171–179, 2018, doi: 10.1016/j.jallcom.2018.06.177.

[22]L. Kang, F. Chen, B. Wu, X. Liu, and H. Ge, “Mechanical properties and microstructure of laser-cladding additively manufactured 316L stainless steel sheets,” J. Constr. Steel Res., vol. 199, no. December 2021, p. 107603, 2022, doi: 10.1016/j.jcsr.2022.107603.

[23]M. Zhao, H. Wu, J. Lu, G. Sun, and L. Du, “Materials Characterization Effect of grain size on mechanical property and corrosion behavior of a metastable austenitic stainless steel,” Mater. Charact., vol. 194, no. September, p. 112360, 2022, doi: 10.1016/j.matchar.2022.112360.

[24]S. Rangrej, S. Pandya, and J. Menghani, “Effects of reinforcement additions on properties of aluminium matrix composites - A review,” Mater. Today Proc., vol. 44, pp. 637–641, 2021, doi: 10.1016/j.matpr.2020.10.604.

[25]F. Chen et al., “Tribological behavior and mechanism of h-BN modified copper metal matrix composites paired with C/C–SiC,” Tribol. Int., vol. 153, no. July 2020, 2021, doi: 10.1016/j.triboint.2020.106561.

[26]Y. C. Wu et al., “The superior properties of spark plasma sintered La-Fe-Si magnetocaloric alloys,” Mater. Res. Bull., vol. 155, no. July, p. 111974, 2022, doi: 10.1016/j.materresbull.2022.111974.

[27]Z. Hu, Z. Zhang, X. Cheng, F. Wang, Y. Zhang, and S. Li, “A review of multi-physical fi elds induced phenomena and effects in spark plasma sintering : Fundamentals and applications,” vol. 191, 2020.

[28]S. Ali et al., “Microstructure and Mechanical Properties of Modified 316L Stainless Steel Alloy for Biomedical Applications Using Powder Metallurgy,” 2022.

[29]C. K. F. Fang, “State of the art of bioimplants manufacturing : part II,” Adv. Manuf., vol. 6, no. 2, pp. 137–154, 2018, doi: 10.1007/s40436-018-0218-9.

[30]A. Azeez et al., “A Review of Additive Mixed-Electric Discharge Machining : Current Status and Future Perspectives for Surface Modification of Biomedical Implants,” vol. 2017, 2017, doi: 10.1155/2017/8723239.

[31]C. K. F. Fang, “State of the art of bioimplants manufacturing : part I,” Adv. Manuf., vol. 6, no. 1, pp. 20–40, 2018, doi: 10.1007/s40436-017-0207-4.

[32]E. Mardaras and I. Fern, “Influence of Severe Surface Plastic Deformation Induced by Shot Peening on Microstructure and Corrosion Resistance of fine grained 316 L stainless steel,” vol. 231, no. January, 2024, doi: 10.1016/j.corsci.2024.111988.

[33]X. Yue, Z. Yang, L. Huang, L. Zhang, J. Li, and Z. Xue, “Journal of Materials Science & Technology Passivation characteristics of ultra-thin 316L foil in NaCl solutions,” J. Mater. Sci. Technol., vol. 127, pp. 192–205, 2022, doi: 10.1016/j.jmst.2022.01.043.

[34]S. Robi, X. Wang, M. Brochu, and S. Omanovic, “Effects of crystallographic orientation on the corrosion behavior of stainless steel 316L manufactured by laser powder bed fusion,” Corros. Sci., vol. 196, no. September 2021, p. 110009, 2022, doi: 10.1016/j.corsci.2021.110009.

[35]A. Racot, I. Aubert, M. Touzet, and M. Demesy, “Statistical analysis of the pitting corrosion induced by potentiostatic pulse tests of wrought and SLM 316L stainless steels,” vol. 197, no. October 2020, 2022, doi: 10.1016/j.corsci.2021.110036.

[36]J. Choi, G. Lee, J. Song, W. Lee, and J. Lee, “Sintering behavior of 316L stainless steel micro – nanopowder compact fabricated by powder injection molding,” Powder Technol., vol. 279, pp. 196–202, 2015, doi: 10.1016/j.powtec.2015.04.014.

[37]E. Liu, “E ff ect of strain-induced martensite on the tribocorrosion of AISI 316L austenitic stainless steel in seawater,” pp. 44923–44932, 2017, doi: 10.1039/c7ra07318f.

[38]Q. He et al., “Microstructure and properties of 316L stainless steel foils for pressure sensor of pressurized water reactor,” Nucl. Eng. Technol., vol. 53, no. 1, pp. 172–177, 2021, doi: 10.1016/j.net.2020.06.006.

[39]A. Parveen, N. R. Chauhan, and M. Suhaib, “Mechanical and tribological behaviour of Al-ZrO2 composites: A review,” Lect. Notes Mech. Eng., pp. 217–229, 2019, doi: 10.1007/978-981-13-6469-3_20.

[40]E. E. Feldshtein, L. N. Dyachkova, and J. Patalas-Maliszewska, “On investigating the microstructural, mechanical, and tribological properties of hybrid feGr1/Sic/Gr metal matrix composites,” Materials (Basel)., vol. 14, no. 1, pp. 1–12, 2021, doi: 10.3390/ma14010174.

[41]S. Sahoo, S. Samal, and B. Bhoi, “Fabrication and characterization of novel Al-SiC-hBN self-lubricating hybrid composites,” Mater. Today Commun., vol. 25, no. March, p. 101402, 2020, doi: 10.1016/j.mtcomm.2020.101402.